Available online at www.sciencedirect.com

SciVerse ScienceDirect

www.elsevier.com/locate/jprot

Effect of high glucose on secreted proteome in cultured retinal pigmented epithelium cells: Its possible relevance to clinical diabetic retinopathy

You-Hsuan Chen[a], Hsiu-Chuan Chou[b], Szu-Ting Lin[a], Yi-Wen Chen[a], Yi-Wen Lo[b], Hong-Lin Chan[a,*]

[a]Institute of Bioinformatics and Structural Biology & Department of Medical Sciences, National Tsing Hua University, Hsinchu, Taiwan
[b]Department of Applied Science, National Hsinchu University of Education, Hsinchu, Taiwan

ARTICLE INFO

Article history:
Received 24 February 2012
Accepted 4 July 2012
Available online 16 July 2012

Keywords:
Proteomics
Secretomics
Retinal pigmented epithelium cells
2D-DIGE
MALDI-TOF MS

ABSTRACT

Retinopathy has been observed in around quarter of diabetic patients. Diabetic retinopathy can result in poor vision and even blindness since high glucose has been evidenced to weaken retinal capillary leading to leakage of blood into the surrounding space. In the present study, a proteomics-based approach has been applied to analyze a model retinal pigmented epithelium cell line, ARPE-19, grown in mannitol-balanced 5.5 mM, 25 mM and 100 mM D-glucose culture media and used as a model for hyperglycemia secretomic analysis. Totally, 55 differentially secreted proteins have been firmly identified representing 46 unique gene products. These secreted proteins mainly function in cytoskeleton-associated adhesion/junction (such as galectin-3-binding protein) and transport (multidrug resistance-associated protein 1). Additionally, the identified secreted markers including asialoglycoprotein receptor 1, lysophosphatidic acid receptor 3, moesin, MPP2, haptoglobin and cathepsin D were further validated in plasma samples coming from type 2 diabetic patients with retinopathy and healthy donors. In summary, we report a comprehensive retinal cell-based proteomic approach for the identification of potential secreted retinal markers-induced in high glucose conditions. Some of these identified secreted proteins have been validated in diabetic retinopathy plasma demonstrating the potentially utilizing of these markers in screening and treating diabetic retinopathy.

1. Introduction

The retina, a light-sensitive tissue, is the nerve layer which could construct images of objects and locate at the backside of eye. These specialized cells are able to survive by means of obtaining their nutrients and oxygen from adjacent tiny blood vessels. Diabetic retinopathy is a disease of the retina, observing in around one fourth of diabetic patients [1,2]. Diabetic retinopathy can cause weak vision and even blindness while high blood glucose has been evidenced to weaken retinal capillary resulting in leakage of blood into the surrounding space. This hemorrhage can also cause the

Abbreviations: 1-DE, one-dimensional gel electrophoresis; 2-DE, two-dimensional gel electrophoresis; Ab, antibody; CCB, colloidal coomassie blue; CHAPS, 3-[(3-cholamidopropyl)-dimethylammonio]-1-propanesulfonate); ddH_2O, double deionized water; DIGE, differential gel electrophoresis; DTT, dithiothreitol; FCS, fetal calf serum; MALDI-TOF MS, matrix assisted laser desorption ionization-time of flight mass spectrometry; NP-40, Nonidet P-40; TFA, trifluoroacetic acid.

* *Corresponding author at:* Institute of Bioinformatics and Structural Biology & Department of Medical Sciences, National Tsing Hua University, Hsinchu, Taiwan. Tel.: +886 3 5742476; fax: +886 3 5715934.
E-mail address: hlchan@life.nthu.edu.tw (H.-L. Chan).

1874-3919/$ – see front matter © 2012 Elsevier B.V. All rights reserved.
doi:10.1016/j.jprot.2012.07.014

formation of scar which can pull on the retina and cause the retina to detach from the wall of the eye. Additionally, hyperglycemia of diabetic retinopathy is possibly to cause macular edema due to the damages in blood-retinal barrier which results in leakage of blood proteins to make macular thicken, swell and ultimately distorted a patient's central vision. However, the detail molecular mechanisms and the diagnostic biomarkers of the disease are largely waiting for elucidation [3–7].

Two-dimensional gel electrophoresis (2-DE) and MALDI-TOF MS have been widely used for profiling plasma proteins. And some of the nonionic and zwitterionic detergents such as CHAPS have been used to improve the solubility of the hydrophobic proteins. Moreover, a significant progression of gel-based analysis of protein quantifications and detections is the introduction of fluorescent 2D-DIGE. 2D-DIGE is able to co-detect numerous samples in the same 2-DE to minimize gel-to-gel variation and compare the protein features across different gels by means of an internal fluorescent standard. This innovative strategy relies on the pre-labeling of protein samples before electrophoresis with fluorescent dyes Cy2, Cy3 and Cy5 each exhibiting a distinct fluorescent wavelength to allow multiple experimental samples to include an internal standard. Thus, the samples can be concomitantly separated in one gel. The internal standard, which is a pool of an equal amount of the experimental protein samples, can facilitate the data accuracy in normalization and increase statistical confidence in relative quantity across gels [8–12].

In this study, developing a proteomic plateform to monitor diabetic retinopathy is crucial for both diagnosis and eventual prognosis. Although recent serum proteomic studies of diabetic cases have identified several putative diabetic biomarkers, the dominant problem with plasma is its complexity and the large dynamic range of individual protein concentrations in plasma. The high abundant proteins are likely to mask low-abundant proteins and complicate their detection. Thus, our strategy was choosing a model retinal pigmented epithelium cell line, ARPE-19, which has been chosen as a cell model for blood-retinal barrier, age-related macular degeneration and diabetic retinopathy associated studies [13–15] to maintain this cell line in mannitol-balanced 5.5 mM, 25 mM and 100 mM D-glucose culture media, respectively, and used as a model for hyperglycemia proteomic analysis. The identified hyperglycemia-related secreted markers were further validated in plasma samples coming from healthy donors and type 2 diabetic patients with retinopathy.

2. Materials and methods

2.1. Chemicals and reagents

Generic chemicals and albumin and IgG depletion kit were purchased from Sigma–Aldrich (St. Louis, USA), while reagents and Cy2/Cy3/Cy5 dyes for 2D-DIGE were purchased from GE Healthcare (Uppsala, Sweden). All the chemicals and biochemicals used in this study were of analytical grade. All the primary antibodies used in this study were purchase from GeneTex (Hsinchu, Taiwan).

2.2. Plasma sample collection and purification

Thirty donors in a single hospital (Chiayi Christian Hospital, Chiayi, Taiwan) were enrolled in the study. Those included in the study were divided into diabetic retinopathy patients (n=15) and healthy donors (n=15) with similar ages (50–60 years old). The criteria to assess the presence of diabetic retinopathy or not were based on the pathological diagnosis and guidelines proposed by the World Health Organization. Diabetic retinopathy individuals were selected with significant retinopathy occurrence more than 5 years after diabetes diagnosed with ages between 50 and 60 years old. In contrast, healthy individuals were selected for healthy donors without diagnosed retinopathy and diabetes with ages between 50 and 60 years old. This study was approved by the Institutional Research Board and carried out according to the Helsinki Declaration Principles. Written informed consent was collected from all participating subjects.

2.3. Cell lines and cell cultures

The cell line ARPE-19 was purchased from the American Type Culture Collection (Manassas, VA) and was maintained in Dulbecco's Modified Eagle's medium (DMEM) supplemented with 10% (v/v) fetal calf serum (FCS), L-glutamine (2 mM), streptomycin (100 μg/mL), and penicillin (100 IU/mL) (all from Gibco-Invitrogen Corp., UK). ARPE-19 cells were incubated at 37 °C and 5% CO_2.

For cell culturing at differential glucose concentrations, the cultures were exposed to D-glucose at a final concentration of 25 and 100 mM (corresponding to 2 h after meal plasma glucose level of diabetic patients and glucose level in uncontrolled diabetic patients [16], respectively) and compared with cultures exposed to 5.5 mM D-glucose as control (corresponding to fasting plasma glucose level of diabetes-free people) [17,18]. To exclude the possible effects of hyperosmotic stress, mannitol was used to balance the differential glucose concentrations according to a previous report [19]. After exposure for at least 3 weeks, the monolayer cultures were used for further analysis.

For secreted protein analysis, approximately 1.25×10^8 cells were seeded into twenty-five 175-cm^2 cell culture plates for each cell condition. After 2 days of incubation, the DMEM media were discarded, and the cells were rinsed three times with PBS. Subsequently, 375 ml of serum-free DMEM media was added for an additional 48 h. The media were collected and filtered with 0.45 μm microfilters to remove cell debris and then concentrated 1000-fold with 10-kDa molecular mass cutoff concentrators (Millipore). The concentrated media were then precipitated by adding 1 volume of 100% TCA (at −20 °C) to 4 volumes of sample and incubated for 10 min at 4 °C. The precipitated protein was then recovered by centrifugation at 13,000 rpm for 10 min, and the resulting pellets were washed twice with ice-cold acetone. Air-dried pellets were resuspended in 2-DE lysis buffer for protein quantification.

2.4. MTT cell viability assay

ARPE-19 cells maintaining in mannitol-balanced 5.5 mM, 25 mM and 100 mM glucose, respectively, for at least 3 weeks were trypsinized, counted using a haemocytometer and 5000

cells/well were seeded into 96-well plates. The culture was then incubated in mannitol-balanced 5.5 mM, 25 mM and 100 mM glucose for 24 h followed by removal of the medium. 50 μL of MTT working solution (1 mg/mL) (Sigma) was added to the cells in each well, followed by a further incubation at 37 °C for 4 h. The supernatant was carefully removed; 100 μL of DMSO was added to each well and the plates shaken for 20 min. The absorbance of samples was then measured at a wavelength of 540 nm in a multi-well plate reader. Values were normalized against the untreated samples and were averaged from 8 independent measurements.

2.5. Flow cytometry analysis for apoptosis detection

Annexin-V/propidium iodide (PI) double assay was performed using the Annexin V, Alexa Fluor® 488 Conjugate Detection kit (Life technologies). Following ARPE-19 growing in differential glucose concentration media, cells were typsinized from culture dish and washed twice with cold PBS. 1×10^6 cells were resuspended in 500 μL binding buffer and stained with 5 μL Alexa Fluor 488 conjugated annexin V according to the manufacturer's instructions. 1 μL 100 μg/mL propidium iodide (PI) was added and mixed gently to incubate with cells for 15 min at room temperature in the dark. After incubation period, samples were subjected to FCM analysis in 1 h using BD Accuri C6 Flow Cytometry (BD Biosciences, San Jose, CA). The data were analyzed using Accuri CFlow@ and CFlow Plus analysis software (BD Biosciences).

2.6. 2D-DIGE and image analysis

For 2D-DIGE analysis, protein samples were labeled with N-hydroxysuccinimidyl ester-derivatives of the cyanine dyes Cy2, Cy3 and Cy5 following the protocol described previously [20,21]. Briefly, 150 μg of protein sample was minimally labeled with 375 pmol of either Cy3 or Cy5 for comparison on the same 2-DE. To facilitate image matching and cross-gel statistical comparison, a pool of all samples was also prepared and labeled with Cy2 at a molar ratio of 2.5 pmol Cy2 per μg of protein as an internal standard for all gels. The labeling reactions were performed in the dark on ice for 30 min and then quenched with a 20-fold molar ratio excess of free L-lysine to dye for 10 min. The differentially Cy3- and Cy5-labeled samples were then mixed with the same amount of Cy2-labeled internal standard and reduced with 65 mM dithiothreitol for 10 min. IPG buffer, pH 3–10 nonlinear (2% (v/v), GE Healthcare) was added and the final volume was adjusted to 450 μL with 2D-lysis buffer for rehydration. Immobilized pH gradient (IPG) strips (pH 3–10 NL, 24 cm) were rehydrated with the CyDye-labeled samples in the dark at room temperature overnight. Isoelectric focusing was then performed using a Multiphor II apparatus (GE Healthcare) for a total of 62.5 kVh at 20 °C. Strips were equilibrated in 6 M urea, 30% (v/v) glycerol, 1% SDS (w/v), 100 mM Tris–HCl (pH 8.8) with 65 mM dithiothreitol for 15 min and then in the same buffer containing 240 mM iodoacetamide for a further 15 min. The equilibrated IPG strips were transferred onto 24×20 cm 12.5% polyacrylamide gels casted between low fluorescent glass plates. The strips were overlaid with 0.5% (w/v) low melting point agarose in running buffer containing bromophenol blue. The gels were run in an Ettan Twelve gel tank (GE Healthcare) at 4 W per gel at 10 °C until the dye front had completely run off the bottom of the gels. Afterward, gels were scanned directly between the glass plates using an Ettan DIGE Imager (GE Healthcare). Image analysis was performed using DeCyder 2-D Differential Analysis Software v7.0 (GE Healthcare) to co-detect, normalize and quantify the protein features in the images. Features detected from non-protein sources were filtered out. Spots displaying a $\geqq$1.5 average-fold increase or decrease in abundance with a p-value <0.05 were selected for protein identification.

2.7. Protein staining

Colloidal coomassie blue G-250 staining was used to visualize CyDye-labeled protein features in 2-DE. Bonded gels were fixed in 30% v/v ethanol, 2% v/v phosphoric acid overnight, washed three times (30 min each) with ddH_2O and then incubated in 34% v/v methanol, 17% w/v ammonium sulphate, 3% v/v phosphoric acid for 1 h, prior to adding 0.5 g/l coomassie blue G-250. The gels were then left to stain for 5–7 days. No destaining step was required. The stained gels were then imaged on an ImageScanner III densitometer (GE Healthcare), which processed the gel images as .tif files.

2.8. In-gel digestion

Excised post-stained gel pieces were washed three times in 50% acetonitrile, dried in a SpeedVac for 20 min, reduced with 10 mM dithiothreitol in 5 mM ammonium bicarbonate pH 8.0 for 45 min at 50 °C and then alkylated with 50 mM iodoacetamide in 5 mM ammonium bicarbonate for 1 h at room temperature in the dark. The gel pieces were then washed three times in 50% acetonitrile and vacuum-dried before reswelling with 50 ng of modified trypsin (Promega) in 5 mM ammonium bicarbonate. The pieces were then overlaid with 10 μl of 5 mM ammonium bicarbonate and trypsinized for 16 h at 37 °C. Supernatants were collected, peptides were further extracted twice with 5% trifluoroacetic acid in 50% acetonitrile and the supernatants were pooled. Peptide extracts were vacuum-dried, resuspended in 5 μl ddH_2O, and stored at −20 °C prior to MS analysis.

2.9. Protein identification by MALDI-TOF MS

Extracted proteins were cleaved with a proteolytic enzyme to generate peptides, then a peptide mass fingerprinting (PMF) database search following MALDI-TOF MS analysis was employed for protein identification. Briefly, 0.5 μl of tryptic digested protein sample was first mixed with 0.5 μl of a matrix solution containing α-cyano-4-hydroxycinammic acid at a concentration of 1 mg in 1 ml of 50% acetonitrile (v/v)/0.1% trifluoroacetic acid (v/v), spotted onto an anchorchip target plate (Bruker Daltonics) and dried. The peptide mass fingerprints were acquired using an Autoflex III mass spectrometer (Bruker Daltonics) in reflector mode. The algorithm used for spectrum annotation was SNAP (**S**ophisticated **N**umerical **A**nnotation **P**rocedure). This process used the following detailed metrics: Peak detection algorithm: SNAP; Signal to noise threshold: 25; relative intensity threshold: 0%; minimum intensity threshold: 0; maximal number of peaks: 50;

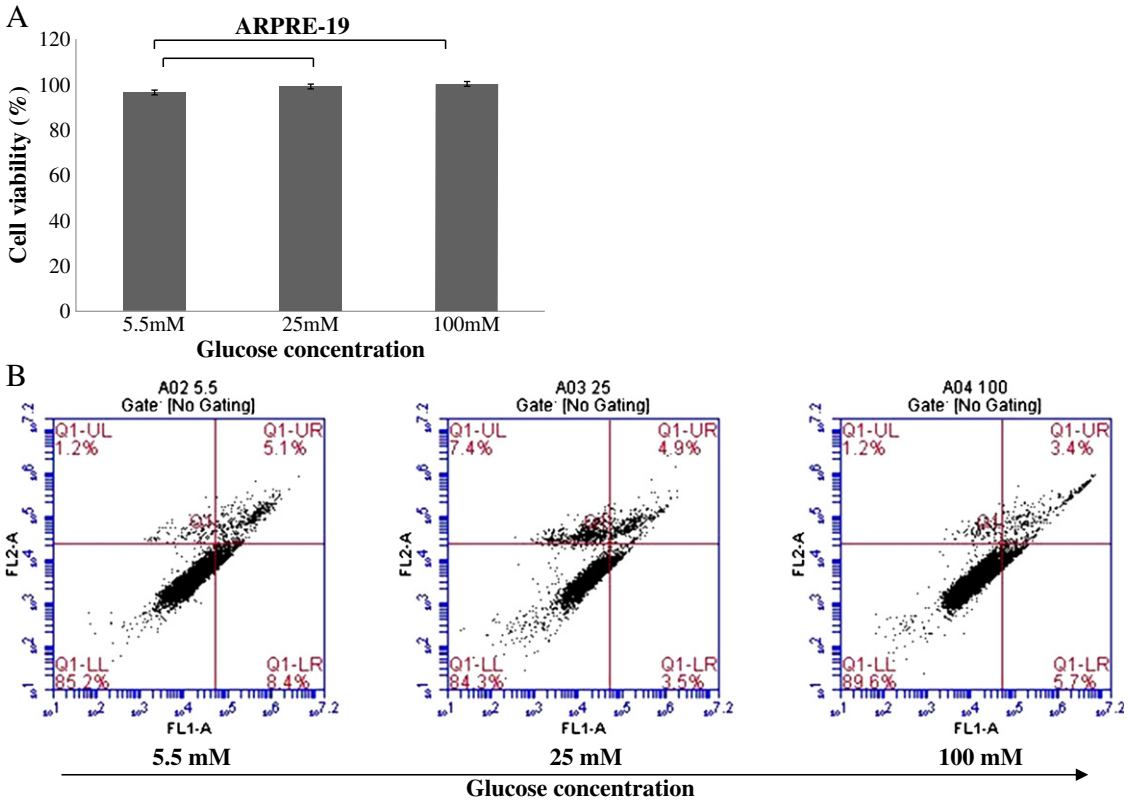

Fig. 1 – Effect of glucose concentration on cell viability and cell apoptosis in ARPE-19. (A) MTT-based viability assays were performed on ARPE-19 cell cultures following 3 weeks at different glucose concentrations (5.5 mM, 25 mM and 100 mM glucose). Values were normalized against 5.5 mM samples and are the average of 3 independent measurements +/– the standard deviation. (B) 10^6 different glucose concentrations cultured ARPE-19 cells were incubated with Alexa Fluor 488 and propidium iodide in 1x binding buffer at room temperature for 15 min, and then stained cells were analyzed by flow cytometry to examine effect of different glucose concentrations on apoptosis in APRE-19 cells. Annexin V is presented in x-axis as FL1-H, and propidium iodide is presented in y-axis as FL2-H. LR quadrant indicates the percentage of early apoptotic cells (Annexin V positive cells), and UR quadrant indicates the percentage of late apoptotic cells (Annexin V positive and propidium iodide positive cells).

quality factor threshold: 1000; SNAP average composition: averaging; baseline subtraction: median; flatness: 0.8; MedianLevel: 0.5. The spectrometer was also calibrated with a peptide calibration standard (Bruker Daltonics) and internal calibration was performed using trypsin autolysis peaks at *m/z* 842.51 and *m/z* 2211.10. Peaks in the mass range of *m/z* 800–3000 were used to generate a peptide mass fingerprint that was searched against the Swiss-Prot/TrEMBL database (2010_12, 515203 sequence entries) using Mascot software v2.3.00 (Matrix Science, London, UK). The following parameters were used for the search: *Homo sapiens*; tryptic digest with a maximum of 1 missed cleavage; carbamidomethylation of cysteine, partial protein N-terminal acetylation, partial methionine oxidation and partial modification of glutamine to pyroglutamate and a mass tolerance of 50 ppm. Identification was accepted based on significant MASCOT Mowse scores ($p<0.05$), spectrum annotation and observed versus expected molecular weight and p*I* on 2-DE.

2.10. *Immunoblotting*

Immunoblotting was used to validate the differential abundance of mass spectrometry identified proteins. Aliquots of

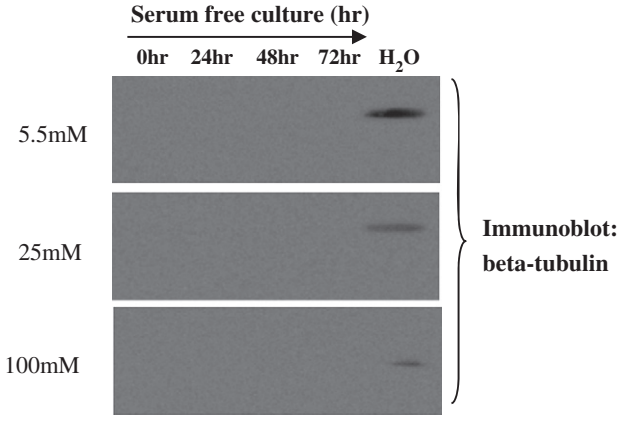

Fig. 2 – Optimization of starvation time for secreted proteomic analysis. ARPE-19 incubated in 5.5 mM, 25 mM and 100 mM glucose for at least 3 weeks followed by incubated in serum free medium for indicated periods were used to check starvation induced cell autolysis by detecting the release of cytoplasmic proteins, β-tubulin, in serum-free media. The serum-free media were harvested and concentrated for 1000-fold at indicative starvation periods prior to performing immunoblotting analysis.

20 μg of purified cell lysates or plasma proteins were diluted in Laemmli sample buffer (final concentrations: 50 mM Tris pH 6.8, 10% (v/v) glycerol, 2% SDS (w/v), 0.01% (w/v) bromophenol blue) and separated by 1D-SDS-PAGE following standard procedures. After electroblotting separated proteins onto 0.45 μm Immobilon P membranes (Millipore), the membranes were blocked with 5% w/v skim milk in TBST (50 mM Tris pH 8.0, 150 mM NaCl and 0.1% Tween-20 (v/v)) for 1 h. Membranes were then incubated in primary antibody solution in TBS-T containing 0.02% (w/v) sodium azide for 2 h. Membranes were washed in TBS-T (3×10 min) and then probed with the appropriate horseradish peroxidase-coupled secondary antibody (GE Healthcare). After further washing in TBS-T, immunoprobed proteins were visualized using an enhanced chemiluminescence method (Visual Protein Co.).

2.11. *Enzyme-linked immunosorbent assay (ELISA) analysis of plasma*

EIA polystyrene microtitration wells were coated with 50 μg of protein samples and incubate at 37 °C for 2 h. The plate was washed for three times with phosphate buffered saline-tween

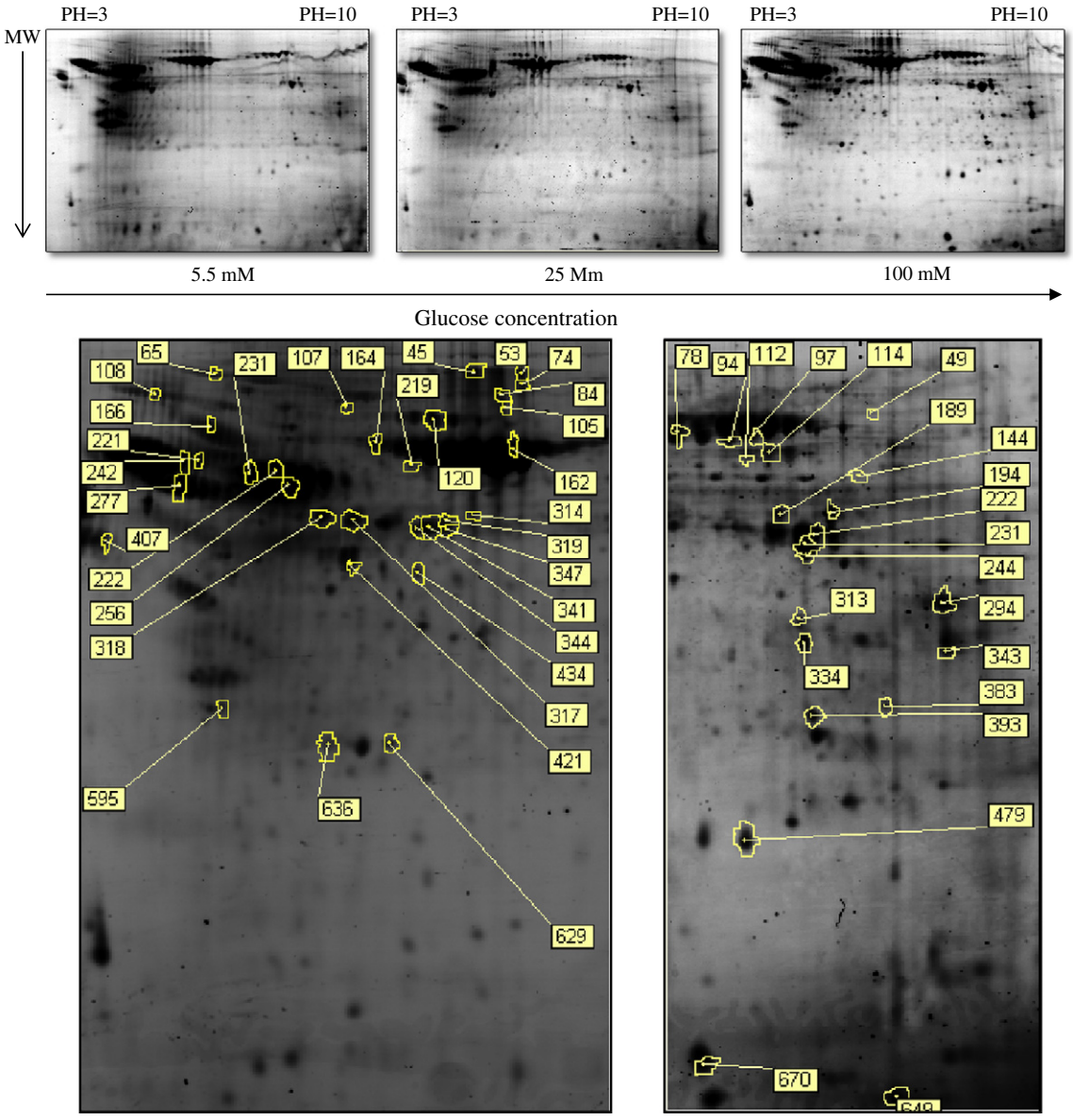

Fig. 3 – Secretomic comparisons across ARPE-19 cells incubated in 5.5 mM, 25 mM and 100 mM glucose using 2D-DIGE. Protein samples (150 μg each) enriched from serum-free media were labeled with Cy-dyes and separated using 24 cm, pH 3–10 non-linear IPG strips. 2D-DIGE images of ARPE-19 incubated in 5.5 mM, 25 mM and 100 mM glucose at appropriate excitation and emission wavelengths were shown. The differentially expressed identified protein features are annotated with spot numbers.

20 (PBST) and three times with PBS. After the uncoated space was blocked with 100 μl of 5% skimmed milk in PBS at 37 °C for 2 h, the plate was washed three times with PBST. Antibody solution was added and incubated at 37 °C for 2 h. After washing with PBST and PBS for 10 times in total, 100 μl of peroxidise-conjugated secondary antibodies in PBS was added for incubation at 37 °C for 2 h. Following 10 washings, 100 μl of 3, 3′, 5, 5′-tetramethyl benzidine (Pierce) was added. After incubation at room temperature for 30 min, 100 μl of 1 M H_2SO_4 was added to stop the reaction followed by measured absorbance at 450 nm using Stat Fax 2100 microtiterplate reader (Awareness Technology Inc. FL, USA).

3. Results

3.1. *Optimization of cell conditions for secreted protein analysis*

In order to examine the effect of high glucose on retinal pigmented epithelium cell, ARPE-19 cells were cultured in 5.5 mM, 25 mM and 100 mM glucose corresponding to fasting plasma glucose level of diabetes-free people, 2 h after meal plasma glucose level of diabetic patients and glucose level in uncontrolled diabetic patients, respectively. For at least 3 weeks incubation, there was no significant change in cell viability, cell

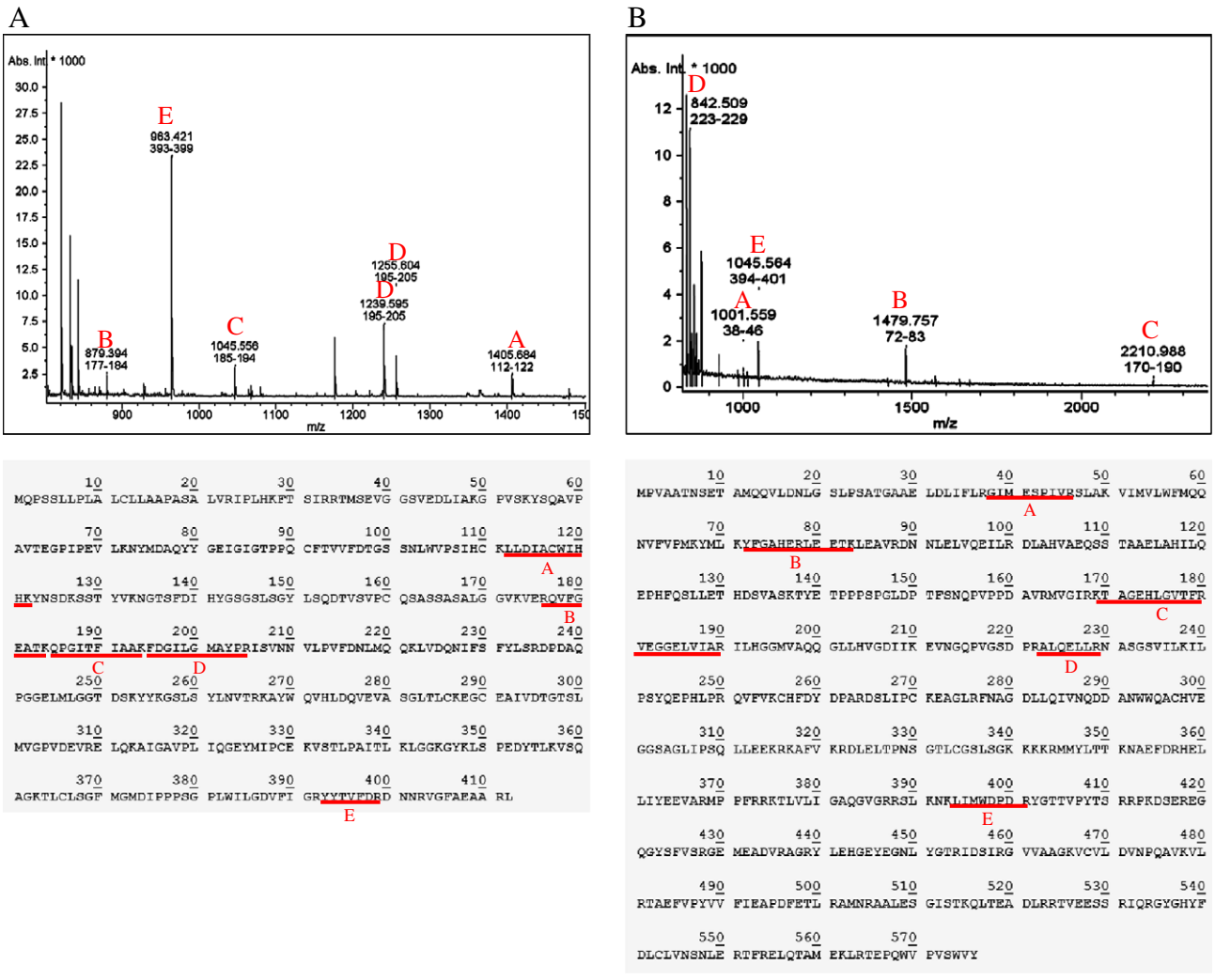

Fig. 4 – Peptide mass fingerprinting of differentially expressed secreted proteins: cathepsin D, MPP2, moesin and haptoglobin. (A) Peptide mass fingerprinting of cathepsin D and its matched peptide sequences (LLDIACWIH, QVFGEATK, QPGITFIAAK, FDGILGM(±oxidation)AYPR, and YYTVFDR), (B) Peptide mass fingerprinting of MPP2 and its matched peptide sequences (GIMESPIVR, YFGAHERLEETK, TAGEHLGVTFRVEGGELVIAR, ALQELLR and LIMWDPDR), (C) Peptide mass fingerprinting of moesin and its matched peptide sequences (LFFLQVK, IQVWHEEHR, IGFPWSEIR, APDFVFYAPR, ALTSELANAR and IDEFESM) and (D) Peptide mass fingerprinting of haptoglobin and its matched peptide sequences (TEGDGVYTLNDKK, KQWINK, QWINKAVGDK, QLVEIEK and HYEGSTVPEK). Mass spectra were acquired on an Autoflex TOF/TOF mass spectrometer (Bruker Daltonics). Peptides contribute to protein identifications were marked with *m/z* values and sequence locations on proteins which were searched against the Swiss-Prot/TrEMBL database (2010_12, 515203 sequence entries) using Mascot software v2.3.00 (Matrix Science, London, UK).

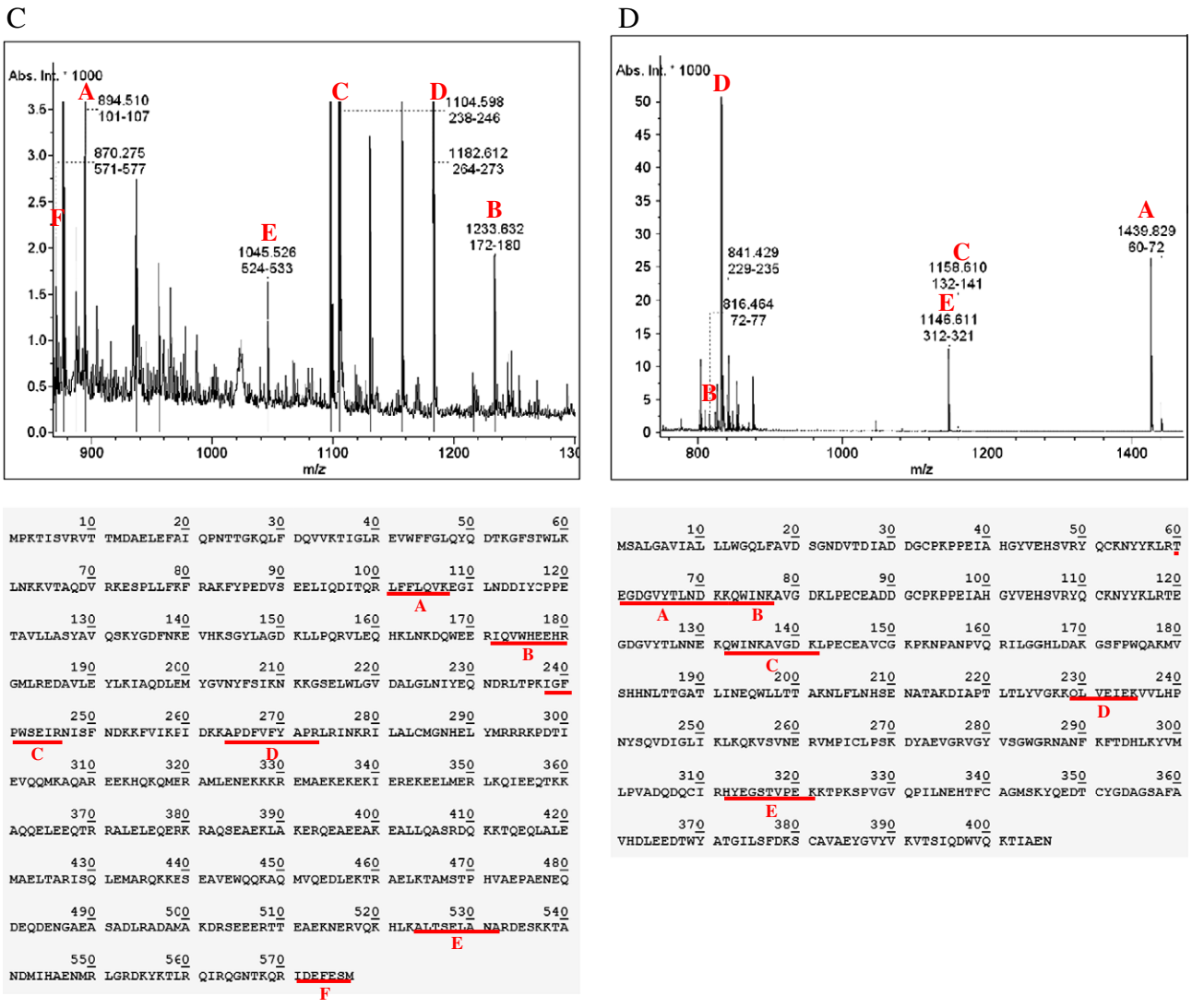

Fig. 4 (*continued*).

apoptosis and cell morphology in any of the culture models as monitored by MTT assay, apoptotic assay and cell imaging, respectively (Fig. 1A, B and supplementary Figure). Subsequent secreted proteomic analysis, ARPE-19 cells were grown in cell culture dishes and the confluency of cells was checked prior to incubation in serum-free culture media to ensure that no other exogenous proteins were present. To minimize cell autolysis induced by starvation and to maximize secreted protein concentration in the media, the starvation time of each cell condition was optimized (refer to Materials and methods). Through immunoblotting, no auto-lysis signal, β-tubulin, was detected in the 1000-fold concentrated serum-free media with starvation periods between 0 and 72 h. In contrast, a significant β-tubulin released was observed for ARPE-19 cells treated with hypotonic H_2O (Fig. 2). β-tubulin is cytoplasmic proteins and their levels in the media represent the amount of cell death taking place in cell culture. Accordingly, a starvation period of 48 h was chosen for further 2D-DIGE based secretomic analysis.

3.2. *2D-DIGE and MALDI-TOF MS analysis of differentially secreted proteome among ARPE-19 grown in 5.5 mM, 25 mM and 100 mM of glucose*

Proteins secreted from each condition were enriched from the serum-free medium followed by labeling with CyDyes for 2D-DIGE analysis. The secretomic profiling of ARPE-19 grown in 5.5 mM, 25 mM and 100 mM of glucose were visualized using a fluorescence scanner and the images were analyzed with DeCyder software (Fig. 3). To investigate the potential involvement of secreted proteins in differential glucose concentrations for retinal pigmented epithelium ARPE-19 cells, biological variation analysis of spots showing greater than 1.5-fold change in expression with a t-test score of less than 0.05 were visually checked before confirming the alterations for protein identification. MALDI-TOF MS identification revealed 55 differentially expressed proteins across differential glucose concentrations (Table 1, Figs. 4 and 5). Of the proteins identified, 50 were differentially expressed between 25 mM/5.5 mM and 48 of

Table 1 – Alphabetical list of identified differentially expressed secreted proteins across ARPE-19 cells incubated in 5.5 mM, 25 mM and 100 mM glucose obtained after 2D-DIGE coupled with MALDI-TOF mass spectrometry analysis. [a]The average ratio of differentially expressed ($p<0.05$) proteins across 25 mM/5.5 mM and 100 mM/5.5 mM glucose concentrations were calculated considering 3 replicate gels. [b,c]The subcellular locations and functional classes of identified proteins were obtained from the Uniprot website (http://www.uniprot.org/). [d]Identified proteins have not been reported in any diabetic retinopathy research.

No.	Swiss-prot no.	Protein name	pI	MW	No. match. peptides	Cov. (%)	Score	25 mM/ 5.5 mM[a]	T-test	100 mM/ 5.5mM[a]	T-test	Subcellular location[b]	Functional Ontology[c]	Match peptide sequences
595	Q04917	14-3-3 protein eta[d]	4.76	28372	4	14	62/56	−1.63	0.013	−1.23	0.3	Cytoplasma	Signal transduction	R.YLAEVASGEK.K;R.LAEQAER.Y
670	P46952	3-hydroxyanthranilate 3,4-dioxygenase[d]	5.62	32707	4	13	60/56	−3.04	0.039	−1.99	0.052	Cytoplasma	Signal transduction	R.QGEIFLLPAR.VK.VMFIGGPNTR.K
434	Q9H0F7	ADP-ribosylation factor-like protein 6	8.72	21559	3	18	59/56	−2.23	0.0054	−2.58	0.014	Plasma membrane	Protein trafficking	R.LSVLLGLK.K;R.LRMVVAK.E
578	P02763	Alpha-1-acid glycoprotein 1[d]	4.93	23725	3	18	66/56	1.16	0.94	1.92	0.049	Secrection	Transport	K.WFYIASAFR.N; K.EQLGEFYEALDCLR.I
383	P51693	Amyloid-like protein 1[d]	5.54	72815	4	4	57/56	−1.48	0.014	−1.42	0.032	Plasma membrane	Neurite outgrowth	R.QMYPELQIAR.V; M.GPASPAARGLSR.R
114	P07306	Asialoglycoprotein receptor 1[d]	5.28	33735	4	15	58/56	−3.65	0.0093	−1.69	0.19	Plasma membrane	Protein trafficking	R.KGPPPPQPLLQR.L; R.TCCPVNWVEHER.S
313	Q13425	Beta-2-syntrophin[d]	9.03	58369	3	6	59/56	−2.49	0.031	−1.97	0.089	Plasma membrane	Cell adhesion	K.SSLTLGLFR.I;K.TYQVAHMK.S
649	Q8NCI6	Beta-galactosidase-1-like protein 3[d]	9.65	75118	5	6	60/56	−2.09	0.03	−2	0.095	Cytoplasma	Metabolism	K.LFQSVSATPLPR.V; K.QEENFMLGR.A
293	P52848	Bifunctional heparan sulfate Ndeacetylase/ N-sulfotransferase 1[d]	8.07	101488	5	6	60/56	−2.87	0.014	−2.46	0.065	Golgi apparatus	Biosynthesis	R.KYPEMDLDSR.A; R.WLSAYHANQILVLDGKLLR.T
341	P07339	Cathepsin D	6.10	45037	6	8	66/56	−2.76	0.018	−3.61	0.009	Lysozome	Protein degradation	K.FDGILGMAYPR.I; K.FDGILGMAYPR.I
317	P07339	Cathepsin D	6.10	45037	11	6	75/56	−2.59	0.0075	−2.96	0.011	Lysozome	Protein degradation	K.FDGILGMAYPR.I; K.FDGILGMAYPR.I
344	P07339	Cathepsin D	6.10	45037	5	11	79/56	−2.04	0.012	−1.83	0.098	Lysozome	Protein degradation	K.QPGITFIAAK.F; K.FDGILGMAYPR.I
347	P07339	Cathepsin D	6.10	45037	6	11	71/56	−1.35	0.2	−1.51	0.024	Lysozome	Protein degradation	K.FDGILGMAYPR.I; K.FDGILGMAYPR.I
256	P07711	Cathepsin L1[d]	5.31	37996	7	12	58/56	−2.88	0.034	−2.92	0.006	Lysozome	Protein degradation	R.LYGMNEEGWR.R; R.QVMNGFQNR.K
62	Q9BXS0	Collagen alpha-1(XXV) chain	8.60	65130	4	9	66/56	−4.46	0.0023	−1.83	0.11	Plasma membrane	Cytoskeleton	K.GAMGEPGPR.G; R.GESGPPGQPGPQGPPGPK.G
421	P35670	Copper-transporting ATPase 2[d]	6.15	158816	4	2	59/56	−2.52	0.0045	−1.13	0.033	Plasma membrane	Transport	K.VSLEQGSATVK.Y; R.AWEPAMK.K319Q6UXH1
319	Q6UXH1	Cysteine-rich with EGF-like domain protein 2[d]	4.15	40333	3	9	63/56	−2.09	0.057	−1.96	0.013	Secrection	Transport	R.NETHSICTACDESCK.T; K.FNQGMVDTAK.K
53	Q93070	Ecto-ADP-ribosyltransferase 4[d]	9.31	36197	5	18	74/56	−2.3	0.021	−1.58	0.08	Plasma membrane	Biosynthesis	R.TPQQYERSFHFK.Y;-.MGPLINR.C
49	O94769	Extracellular matrix protein 2	8.30	80652	5	10	62/56	2.16	0.13	1.41	0.013	Secrection	Cell adhesion	K.LADDGMDR.V;K.GITMYNK.A

108	Q08380	Galectin-3-binding protein	5.13	66202	13	27	167/56	−1.86	0.0013	−2.11	0.013	Secretion	Cell adhesion	K.TLQALEFHTVPFQLLAR.Y; R.IYTSPTWSAFVTDSSWSAR.K
219	Q08380	Galectin-3-binding protein	5.13	66202	19	12	121/56	−2.17	0.0023	−1.69	0.19	Secretion	Cell adhesion	K.SLGWLKSNCR.H; R.KSQLVYQSR.R
79	Q8IUY3	GRAM domain-containing protein 2[d]	8.37	40908	4	10	59/56	−3.12	0.037	−2.72	0.031	Plasma membrane	Cytoskeleton	K.VVIPVVSVQMIK.K; K.YIFVSLLSR.D
407	P00738	Haptoglobin	6.13	45861	5	11	71/56	1.94	0.015	2.12	0.41	Secrection	Hemoglobin binding	K.KQWINK.A;K.QWINKAVGDK.L
334	Q14573	Inositol 1,4,5-trisphosphate receptor type 3[d]	6.05	306820	3	9	71/56	−2.75	0.0015	−3.17	0.0015	Plasma membrane	Signal transduction	K.LLLALMESR.H;K.KAYLQE EER.E
231	Q96GR2	Long-chain-fatty-acid-CoA ligase ACSBG1[d]	5.73	82093	4	6	58/56	−6.51	0.0015	−2.79	0.061	Cytoplasma	Biosynthesis	R.LDADGFLYITGR.L; K.FLSMLLTLK.C
45	Q9UBY5	Lysophosphatidic acid receptor 3	9.63	40786	6	10	63/56	−2.88	0.01	−1.87	0.038	Plasma membrane	Signal transduction	K.DEDMYGTMK.K; K.DEDMYGTMK.K
105	Q14168	MAGUK p55 subfamily member 2 /MPP2[d]	6.32	64882	5	9	57/56	−1.22	0.39	−1.82	0.014	Plasma membrane	Signal transduction	R.ALQELLR.N; K.TAGEHLGVTFRVEGGELVIAR.I
636	Q3SY17	Mitochondrial carrier triple repeat protein2[d]	9.26	34042	4	10	57/56	−1.77	0.047	−1.61	0.26	Mitochondrion	Transport	K.RPPILTSSK.Q;R.QQLYGIK.T
166	P53778	Mitogen-activated protein kinase 12[d]	5.98	42085	5	12	64/56	−3.21	0.0045	−3.11	0.0036	Cytoplasma	Signal transduction	K.GSDHLDQLKEIMK.V; R.IQFLVYQMLK.G
78	P26038	Moesin	6.08	67892	6	9	72/56	−2.71	0.1	−3.89	0.027	Plasma membrane	Cytoskeleton	K.IGFPWSEIR.N;K.APDFVFYAPR.L
343	Q9UQ99	Multidrug resistance-associated protein 1[d]	6.71	172907	6	3	62/56	−3.87	0.00059	−1.8	0.096	Plasma membrane	Transport	R.QMYPELQIAR.V; M.GPASPAARGLSR.R
84	Q9UL56	NADH-cytochrome b5 reductase 3[d]	7.18	34441	4	17	60/56	−2.53	0.016	−1.51	0.038	Mitochondrion	Biosynthesis	K.YPLRLIDR.E; K.GFVDLVIKVYFK.D
120	Q8N0Y3	Olfactory receptor 4N4[d]	9.03	36384	3	12	56/56	−2.18	0.069	−1.81	0.024	Plasma membrane	Olfaction	K.AMSTCTTR.V;R.MLVDFLSEK.K
164	Q9NUI1	Peroxisomal 2,4-dienoyl-CoA reductase[d]	9.38	31100	5	19	62/56	−2.36	0.049	−1.84	0.049	Peroxisome	Redoxregulation	K.AAVDAMTR.H; K.VTASPLQRLGNK.T
393	P18669	Phosphoglycerate mutase 1[d]	6.07	28900	18	4	61/56	−2.17	0.01	−2.07	0.013	Cytoplasma	Glycolysis	R.HYGGLTGLNK.A; R.VLIAAHGNSLR.G
629	Q5UE93	Phosphoinositide 3-kinase regulatory subunit 6[d]	7.57	85060	3	5	58/56	−1.54	0.025	−1.45	0.051	Cytoplasma	Signal transduction	R.MVIAEQNLTNELYPYQER.V; R.DLPTGADELPAPGSPEMER A
231	P05121	Plasminogen activator inhibitor 1	6.68	45088	11	18	82/56	−2.64	0.05	−2.79	0.067	Secrection	Coagulation	K.TPFPDSSTHR.R; K.TPFPDSSTHRR.L
189	P05121	Plasminogen activator inhibitor 1	6.68	45088	7	17	83/56	−2.48	0.039	−2.38	0.024	Secrection	Coagulation	K.GAVDQLTR.L; K.LVQGFMPHFFR.L
224	P05121	Plasminogen activator inhibitor 1	6.68	45088	13	26	111/56	−5.06	0.02	−3.79	0.011	Secrection	Coagulation	K.LVQGFMPHFFR.L; K.DEISTTDAIFVQR.D
221	P05121	Plasminogen activator inhibitor 1	6.68	45088	12	20	75/56	−2.24	0.011	−2.36	0.0083	Secrection	Coagulation	K.LVQGFMPHFFR.L; R.KPLENLGMTDMFR.Q
244	P05121	Plasminogen activator inhibitor1	6.68	45088	10	20	88/56	−2.55	0.042	−2.12	0.074	Secrection	Coagulation	K.QVDFSEVER.A; K.LVQGFMPHFFR.L

(continued on next page)

Table 1 *(continued)*

No.	Swiss-prot no.	Protein name	pI	MW	No. match. peptides	Cov. (%)	Score	25 mM/ 5.5 mM[a]	T-test	100 mM/ 5.5mM[a]	T-test	Subcellular location[b]	Functional Ontology[c]	Match peptide sequences
162	Q6IQ23	Pleckstrin homology domain-containing family A member[d]	9.39	127626	10	7	70/56	−3.68	0.0014	−1.6	0.21	Plasma membrane	Cell adhesion	R.GQQAQPQRAEK.N; K.MSSEERR.A
222	P51164	Potassium-transporting ATPase subunit beta[d]	6.98	33859	4	10	58/56	−2.89	0.0037	−2.69	0.02	Plasma membrane	Transport	MAALQEK.K;K.FLPSNGSAPR.V
194	Q9H9Q9	Protein KIAA1967[d]	5.14	103456	6	6	56/56	−3.37	0.034	−3.2	0.041	Mitochondrion	Apoptosis	R.IQVSSEK.E;K.ADSWVEK.E
65	Q6XPR3	Repetin[d]	6.42	91304	7	10	65/56	−6.63	0.0074	−3.35	0.016	Secretion	Visual system	R.QDGDSHHGQPER.Q; K.DFSFDQSER.Q
107	Q86VW0	SEC14 domain and spectrin repeatcontaining protein 1[d]	4.99	80048	4	4	60/56	−1.36	0.26	−1.79	0.046	Plasma membrane	Transport	.MEASVILPILK.K;R.GFTVIVDGR.
74	Q9P249	Semaphorin-6D	8.77	121050	5	5	62/56	−1.97	0.011	−1.67	0.11	Plasma membrane	Neurogenesis	K.NDMGGSQR.V ;R.HSISAMPK.N
277	Q9NWH7	Spermatogenesis-associated protein 6[d]	8.80	56980	3	6	58/56	−2.72	0.038	−2.71	0.097	Secretion	Development	K.SHRPIFENSMDK.M; K.EDIYLSICVFGQYK.K
49	Q8NBV8	Synaptotagmin-8[d]	9.65	44737	3	8	57/56	2.16	0.13	1.41	0.023	Plasma membrane	Protein trafficking	R.QAADLRPGGTVDPYAR.V; K.VQLMLNQR.K
479	O75558	Syntaxin-11	6.11	33631	3	11	57/56	−2.22	0.014	−2.38	0.016	Golgi apparatus	Protein trafficking	R.GEVIHCK.L; R.AQYNALTLTFQR.A
94	Q96H15	T-cell immunoglobulin and mucin domain-containing protein 4[d]	5.75	42008	4	10	58/56	−5.38	0.019	−2.99	0.053	Plasma membrane	Signal transduction	K.DQCPYSGCK.E; K.TGQMDGIPMSMK.N
112	O43219	Transforming growth factor-beta-induced protein[d]	7.62	75261	8	11	74/56	−2.43	0.028	−1.83	0.11	Secretion	Cell adhesion	R.ILGDPEALR.D; K.DGTPPIDAHTR.N
150	Q96NL1	Transmembrane protein 74[d]	5.12	33888	5	12	66/56	1.65	0.12	1.67	0.029	Plasma membrane	Autophagy	1 K.NINLEQRNR.S;K.QCASTPR.A
144	Q96NL1	Transmembrane protein 74[d]	5.12	33888	5	15	66/56	2.36	0.15	1.98	0.0054	Plasma membrane	Autophagy	R.RIDITLSSVK.C; K.TLQALEFHTVPFQLLAR.Y
318	P21796	Voltage-dependent anion-selective channel protein 1[d]	8.62	30868	4	13	61/56	−2.9	0.013	−4.22	0.0014	Mitochondrion	Apoptosis	M.AVPPTYADLGK.S; K.GYGFGLIK.L

them were differentially expressed between 100 mM/5.5 mM. For example, peptide mass fingerprint profile listed in Fig. 4A contributes to the identification of cathepsin D which shows a 1.35–2.76-fold and 1.51–3.61-fold down-regulated by incubated in 25 mM and 100 mM glucose media in comparison with ARPE-19 cells incubated in 5.5 mM glucose medium, respectively (Fig. 5A). Also, peptide mass fingerprint profile listed in Fig. 4B contributes to the identification of MPP2 which shows a 1.22-fold and 1.82-fold down-regulated by incubated in 25 mM and 100 mM glucose media in comparison with ARPE-19 cells incubated in 5.5 mM glucose medium, respectively (Fig. 5B). Additionally, peptide mass fingerprint profile listed in Fig. 4C contributes to the identification of moesin which shows a 2.71-fold and 3.89-fold down-regulated by incubated in 25 mM and 100 mM glucose media in comparison with ARPE-19 cells incubated in 5.5 mM glucose medium, respectively (Fig. 5C). Moreover, peptide mass fingerprint profile listed in Fig. 4D contributes to the identification of haptoglobin which shows a 1.94-fold and 2.12-fold up-regulated by incubated in 25 mM and 100 mM glucose media in comparison with ARPE-19 cells incubated in 5.5 mM glucose medium, respectively (Fig. 5D). In the three glucose concentrations investigated, 65% of the total proteins identified were extracellular and plasma membrane-anchored proteins (Fig. 6A). Most of the identified proteins were involved in cytoskeleton-associated adhesion/junction and transport (Fig. 6B). To our knowledge, 35 out of these 55 identified spots, including repetin, have not been reported in any diabetic retinopathy related studies. Consequently, these proteins might have the potential to be hyperglycemia associated retinopathy markers. As expected, this 2D-DIGE experiment also identified a number of reported diabetic retinopathy markers, including cathepsin D [22].

With the basis of a Swiss-Prot search and KEGG pathway analysis, numerous potential biological functions of the identified secreted proteins across ARPE-19 grown in 5.5 mM, 25 mM and 100 mM of glucose were determined. Proteins known to regulate biosynthesis, cell adhesion, cytoskeleton, protein degradation, transport and protein trafficking are found to be down-regulated in the secreted fractions of 25 mM and 100 mM glucose-cultured ARPE-19 cells (Fig. 7).

3.3. *Validation of identified proteins in secreted media and diabetic retinopathy plasma by immunoblotting and ELISA*

The secreted proteomic study indentified some of the well-characterized hyperglycemia-modulated proteins such as cathepsin D in culture media. It is essential to validate the levels of the protein in the medium from independent experiments. To this end, comparing the secreted protein levels of cathepsin D, MPP2, moesin and haptoglobin from the differential glucose concentration culture media were validated with immunoblotting and ELISA. The results showed that cathepsin D, MPP2 and moesin down-regulated in both 25 mM and 100 mM glucose in comparison to the levels in 5.5 mM; in contrast, haptoglobin up-regulated in these high glucose condition (Fig. 8). These observations confirmed that cathepsin D, MPP2, moesin and haptoglobin were differentially secreted depending on glucose concentrations in media.

Further study to determine the clinical relevance of the results described above, we used immunoblotting and ELISA to detect the levels of the potential diabetic retinopathy associated proteins (asialoglycoprotein receptor 1, lysophosphatidic acid receptor 3, moesin, MPP2, haptoglobin and cathepsin D) in plasma samples from diabetic retinopathy patients and healthy controls. For example, as shown in Fig. 9A, the 34 kDa of asialoglycoprotein receptor 1, the 41 kDa of lysophosphatidic acid receptor 3 and the 65 kDa of MPP2 were significantly decreased in the plasma of patients with diabetic retinopathy. Additionally, ELISA assays were also performed to verify proteomic results. There were significant increases in the plasma level of haptoglobin in the diabetic retinopathy patients as compared to the healthy controls. In contrast, the level of cathepsin D and moesin were significantly lower in diabetic retinopathy plasma (Fig. 9B). These immunoblotting and ELISA results are consistent with the data from the 2D-DIGE and MALDI-TOF MS, and further suggest that the identified proteins may be employed as potential indicators for the diagnosis of diabetic retinopathy.

4. Discussion

Secreted proteins, extracellular proteins, and plasma membrane bound proteins are known to mediate cell adhesion, cell-cell interactions, cell motility and cell invasion. These proteins have the highest chances of being found in the circulation system, such as blood, and thus serve as sources from which to find important biomarkers involved in diseases [23]. To investigate potential proteins that may be involved in diabetic retinopathy, an approach for preparing secreted proteins from differential glucose concentrations-cultured retinal cell lines with minimal cytosolic protein contamination has been established in this study. Although these cell lines are normally grown in a serum-supplemented media, a serum free conditioned media is essential to prevent serum protein contamination and to allow accurate detection of secreted proteins secreted from these cells. A serum-free medium is believed to affect the growth of cells and the production of secreted proteins; nevertheless, recent reports indicated that the serum-free condition would not significantly affect the composition of the secreted proteins [24,25]. Additionally, it is inevitable to prevent cell death and the release of significant amounts of cytosolic proteins into culture media either in serum-free condition or serum-supplemented medium. Hence, an intensive wash step was required prior to incubating these cells in serum-free media to remove both cytosolic proteins and serum proteins; in the meantime, the incubation time in serum-free media was optimized in advance to diminish serum-free induced autolysis of the cells to enable the recovery of a sufficient amount of secreted proteins for 2D-DIGE analysis. It has been commonly understood that the concentration of secreted proteins was extremely low at approximately 1–2 μg/ml in our study. For this reason, a concentrating step was critical to enrich enough secreted protein for study and a desalt step was also required to perform 2D-DIGE experiment. In this study, a spin-concentrator coupled TCA-acetone precipitation strategy was used for secreted protein enrichment and sample desalting, respectively.

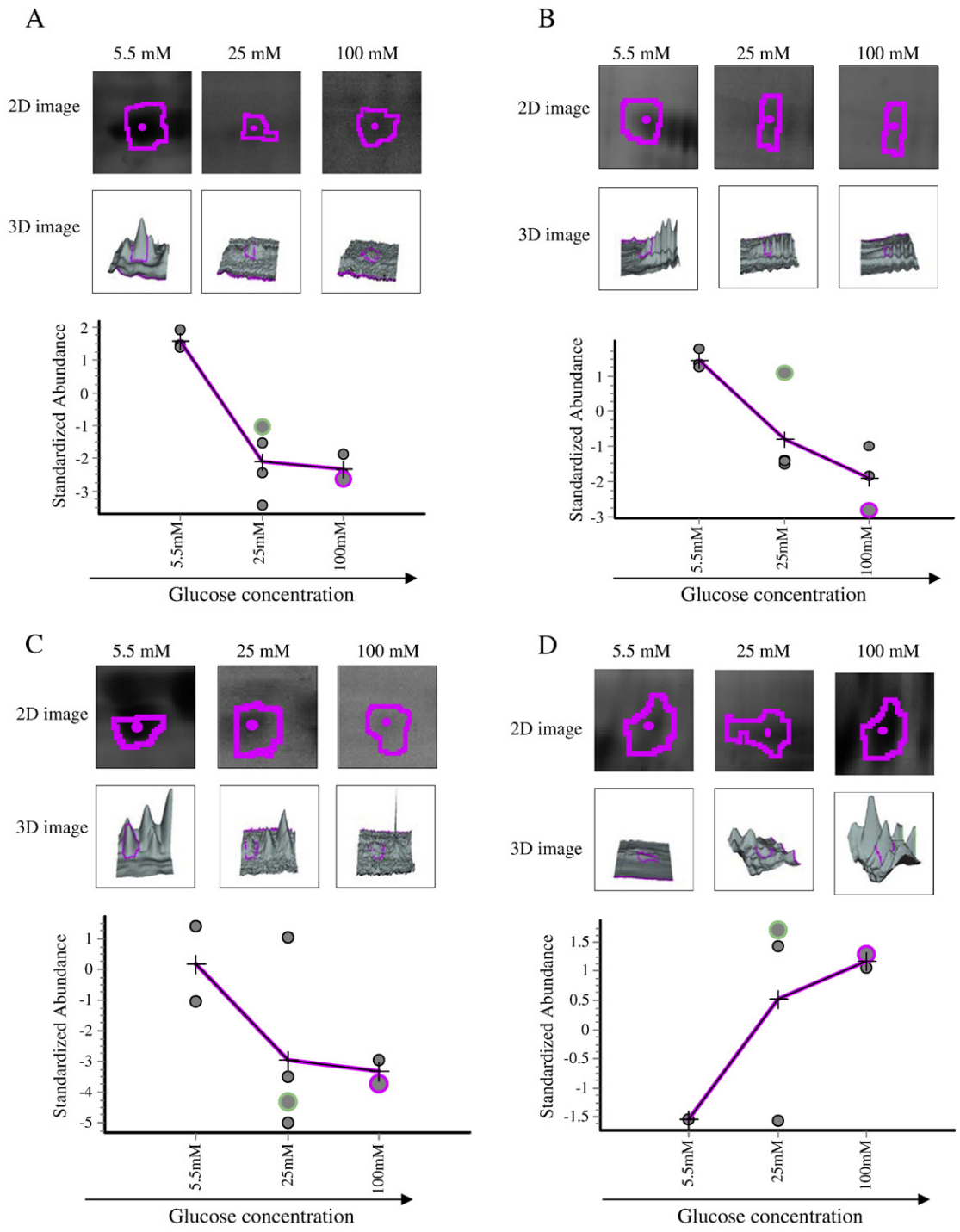

Fig. 5 – Representative images of the identified spots (A) cathepsin D, (B) MPP2, (C) moesin and (D) haptoglobin) displaying high glucose-dependent secreted protein abundance changes. The levels of these secreted proteins were visualized by fluorescence 2-DE images (top panels), three-dimensional spot images (middle panels) and protein abundance map (bottom panels).

After protein separation, quantification and identification by 2D-DIGE and MALDI-TOF mass spectrometry, 35% of the total identified proteins were assigned neither secreted proteins nor membrane-bound proteins. Most of them were sub-located in cytoplasma, implying some levels of cell autolysis or necrosis were taking place. Importantly, 65% of the identified medium proteins were secreted proteins, plasma membrane bound or peripheral proteins, indicating these membrane-associated proteins might be trimmed off the plasma membrane by proteases or not completely integrated into the plasma membrane. The results demonstrated that through our investigation secreted proteins and membrane proteins are significantly enriched in comparison with the only 2% of the entire mammary epithelial cell

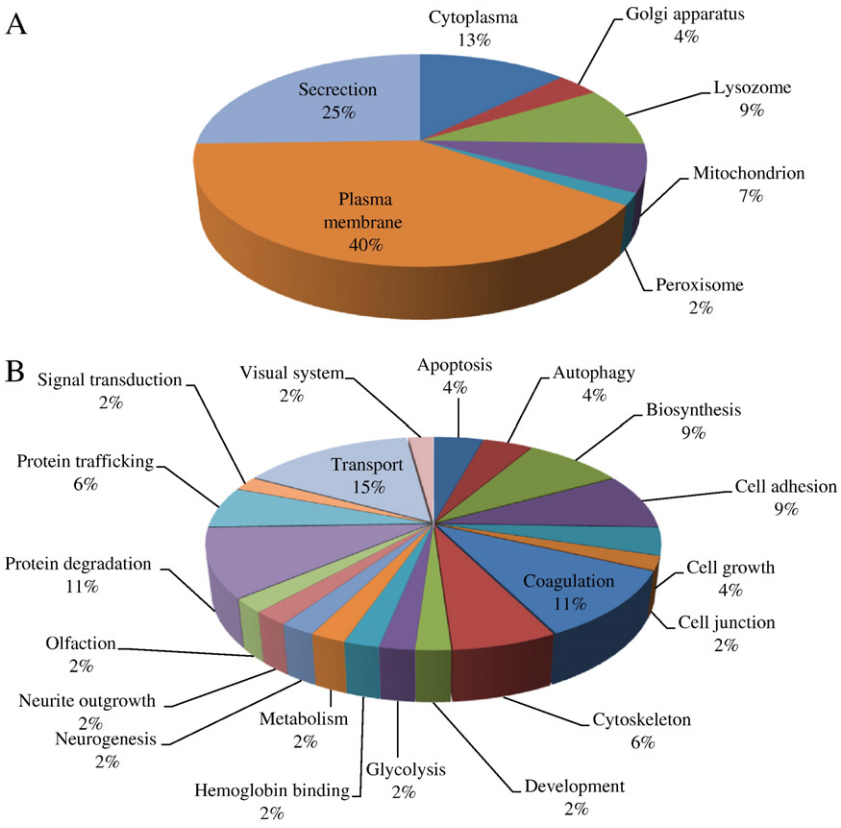

Fig. 6 – Percentage of secreted proteins identified from serum-free media by 2D-DIGE/MALDI-TOF MS for ARPE-19 cells incubated in 5.5 mM, 25 mM and 100 mM glucose according to their sub-cellular locations (A) and biological functions (B).

proteome classified as secreted and plasma membrane proteins [26].

Proteomic analysis of the diseases usually perform a comparative strategy that is defined by the differential expression of the proteins under different disease conditions. Our fluorescent 2D-DIGE-based quantitative proteomic analysis combining MALDI-TOF analysis revealed 55 glucose concentration-dependent secreted proteins corresponding to 46 unique secreted proteins in ARPE-19 cells (Table 1). A majority of altered proteins belong to 5 major functional groups, transport, coagulation, protein degradation, biosynthesis and cell adhesion, while other affected category including protein trafficking and cytoskeleton regulation (Fig. 6B). Of these, protein such as cathepsin D protein has been reported as a diabetic retinopathy regulator and has been suggested that the protein is essential for the metabolic maintenance of retinal photoreceptor cells and that its deficiency induces apoptosis of the retinal cells [27]. In contrast, identified protein such as repetin has not been reported as diabetic retinopathy markers in our knowledge. Further investigation indicated that the combination of these identified proteins have not yet been described as diabetic retinopathy markers. Accordingly, the combination of these identified proteins might be further evaluated as diabetic retinopathy specific markers.

With the basis of a Swiss-Prot search and KEGG pathway analysis, numerous potential biological functions of the identified secreted proteins across ARPE-19 grown in 5.5 mM, 25 mM and 100 mM of glucose were classified. The information should be useful for studying the mechanisms of diabetic retinopathy. Fig. 7 compares the expression profiles of the identified differentially expressed proteins across 3 culture conditions. Proteins known to regulate biosynthesis, cell adhesion, cytoskeleton, protein degradation, transport and protein trafficking are found to be down-regulated in the secreted fractions of 25 mM and 100 mM glucose-cultured ARPE-19 cells.

Biosynthesis plays an essential role in all living cells. Proteomic analysis reveals that proteins involved heparan sulfate synthesis, energy synthesis and fatty acid synthesis are significantly down-regulated in the secreted fractions of 25 mM and 100 mM glucose-cultured ARPE-19 cells. N-sulfotransferase-1 catalyzes the initial modifying step in the biosynthesis of heparan sulphate proteoglycan which is an integral component of retinal epithelial basement membranes. The decrease in heparan sulphate proteoglycan synthesis has been reported to decrease in retinal basement membrane anionic sites and increase capillary permeability that occurs in diabetes [28–31]. These studies and our proteomic analysis demonstrate that high glucose might attenuate the biosynthesis of heparan sulphate proteoglycan via modulate N-sulfotransferase-1 expression leading to capillary permeability of retinal epithelial cells.

Blood vessels damaged from diabetic retinopathy can cause abnormal/fragile blood vessels and leak blood into the center of the eye. In previous studies, numerous adhesion molecules such

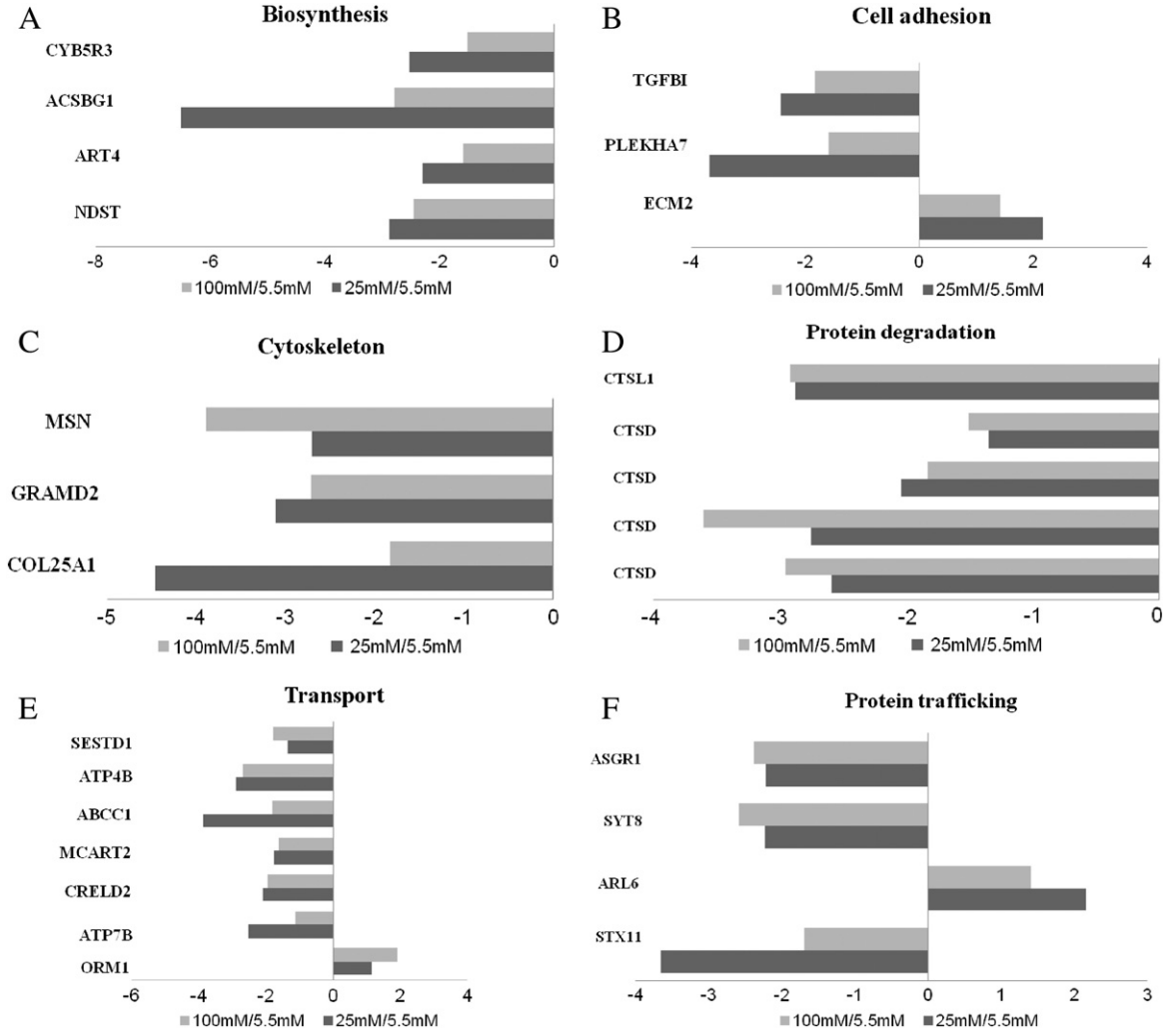

Fig. 7 – Expression profiles for secreted proteins potentially contributing to (A) biosynthesis, (B) cell adhesion, (C) cytoskeleton, (D) protein degradation, (E) transport, (F) protein trafficking in comparing high glucose (25 mM and 100 mM glucose)-cultured ARPE-19 cells with 5.5 mM glucose-cultured ARPE-19. Black bars and gray bars represent fold changes of secreted protein expression in 25 mM and 100 mM glucose-cultured ARPE-19 cells versus 5.5 mM glucose-cultured ARPE-19, respectively. The vertical axis indicates the identified proteins; the horizontal axis indicates the fold change in protein expression. Additional details for each protein can be found in Table 1.

as ICAM-1 and VCAM-1 were reported to be altered expression in diabetic retinopathy and these adhesion molecules are associated with inflammatory-immune process [32–34]. In here, we report four adhesion molecules (beta-2-syntrophin, galectin-3-binding protein, pleckstrin homology domain-containing family A member and transforming growth factor-beta) with significant down-regulation and one up-regulated extracellular protease (extracellular matrix protein 2) in high glucose cultured conditions. Notably, 3 of these identified proteins including beta-2-syntrophin, pleckstrin homology domain-containing family A member and transforming growth factor-beta have not been reported in any diabetic retinopathy studies. Of which, beta-2-syntrophin, an adaptor protein, organizes the subcellular localization of a variety of membrane proteins and links various cell surface receptors to the actin cytoskeleton and the cytoskeleton-associated serine/threonine kinases [35]. Pleckstrin homology domain-containing family A member is required for the maintenance and biogenesis of zonula adherens. This interaction is mediated by KIAA1543/Nezha, which binds microtubules at their minus-ends to adherens junction such as zonula adherens, in turn, modulates epithelial cell-cell junction [36]. Transforming growth factor-beta-induced protein, an adhesion protein, binds to collagens type I, II, and IV and plays an important role in cell-collagen interactions [37]. Moreover, cytoskeleton proteins collagen alpha-1(XXV) chain, GRAM domain-containing protein 2 and moesin were functioned as cytoskeleton-basement/plasma membrane organization [38–40]. The down-regulation of these proteins imply that high glucose might disturb the formation of cytoskeleton-plasma protein/adhesion junction/basement membrane linkages in retinal epithelial cells leading to diabetic retinopathy. Additionally, MAGUK p55 subfamily member 2

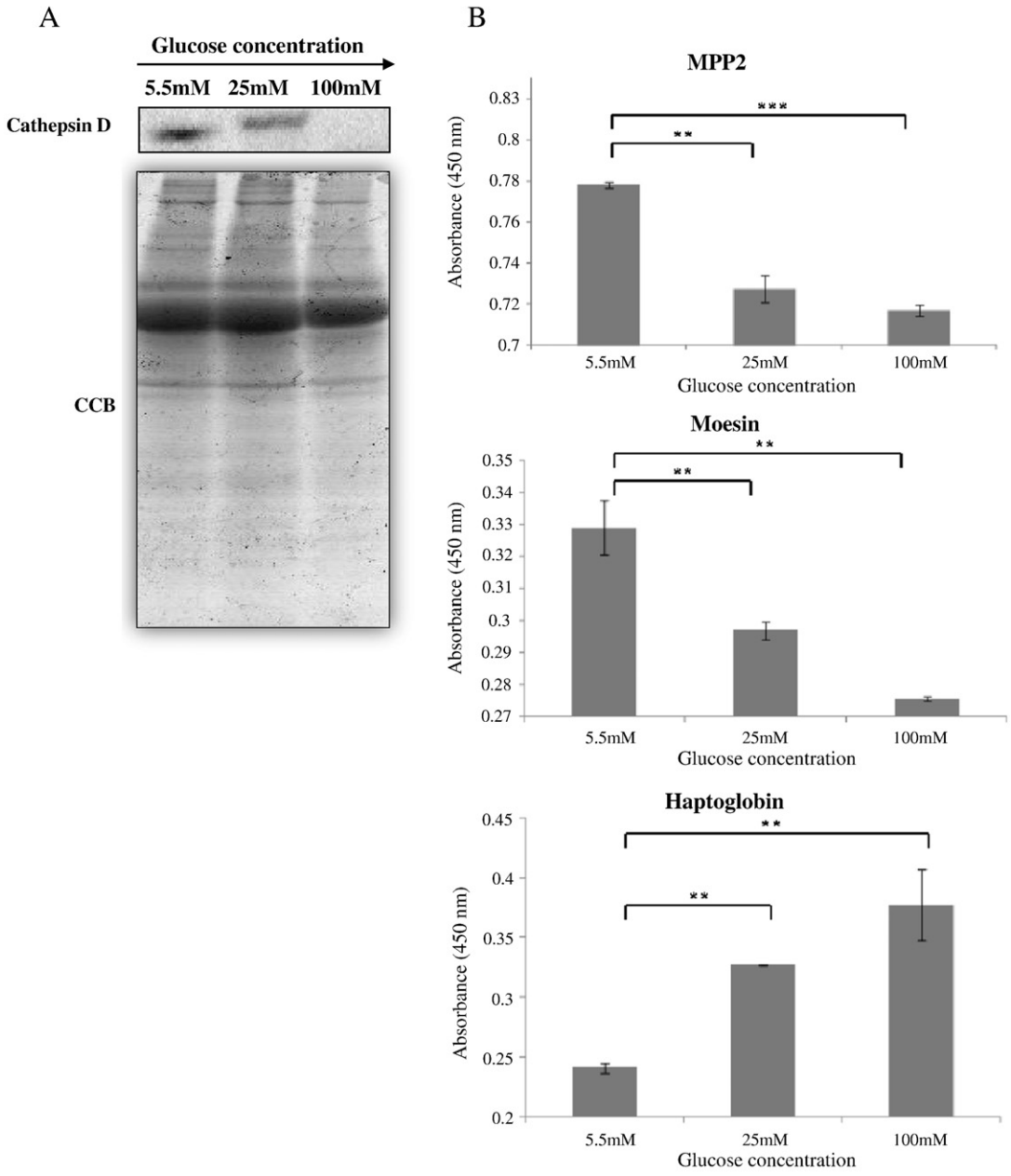

Fig. 8 – Representative immunoblotting and ELISA analyses for selected differentially secreted proteins, cathepsin D, MPP2, moesin and haptoglobin, identified by secreted proteomic analysis in ARPE-19 cells incubated in 5.5 mM, 25 mM and 100 mM glucose. The levels of identified protein, cathepsin D, in serum-free media were confirmed by immunoblotting. Additionally, the level of identified proteins, MPP2, moesin and haptoglobin, were confirmed by ELISA analysis. **Signifies a p-value of ≦ 0.01. * Signifies a p-value of ≦ 0.001.**

(MPP2) is located at the sites of cell–cell contacts with a biological function as cell junction. During cell apoptosis, the protein is a major target for cellular proteases and caspases [41]. Accordingly, the rapid loss of MAGUK in high glucose condition suggests a cell detachment and in the early stage of programmed cell death of ARPE-19 cells. However, the other evidences demonstrate that there are no significant alterations in cell viability (Fig. 1A), cell apoptosis (Fig. 1B) and cell detachment (Supplementary Figure) in these high glucose cultured ARPE-19 cells implying MAGUK protein together with the other biological factors can synergistically contribute to retinal cell apoptosis, detachment and the formation of diabetic retinopathy.

The balance between protein biosynthesis and protein degradation plays an important role in maintaining normal cell physiology. In current proteomic analysis, cathepsin D and cathepsin L1 were both down-regulated in high glucose cultured ARPE-19 cells. Cathepsin D has been reported to be essential for the metabolic maintenance of retinal epithelial

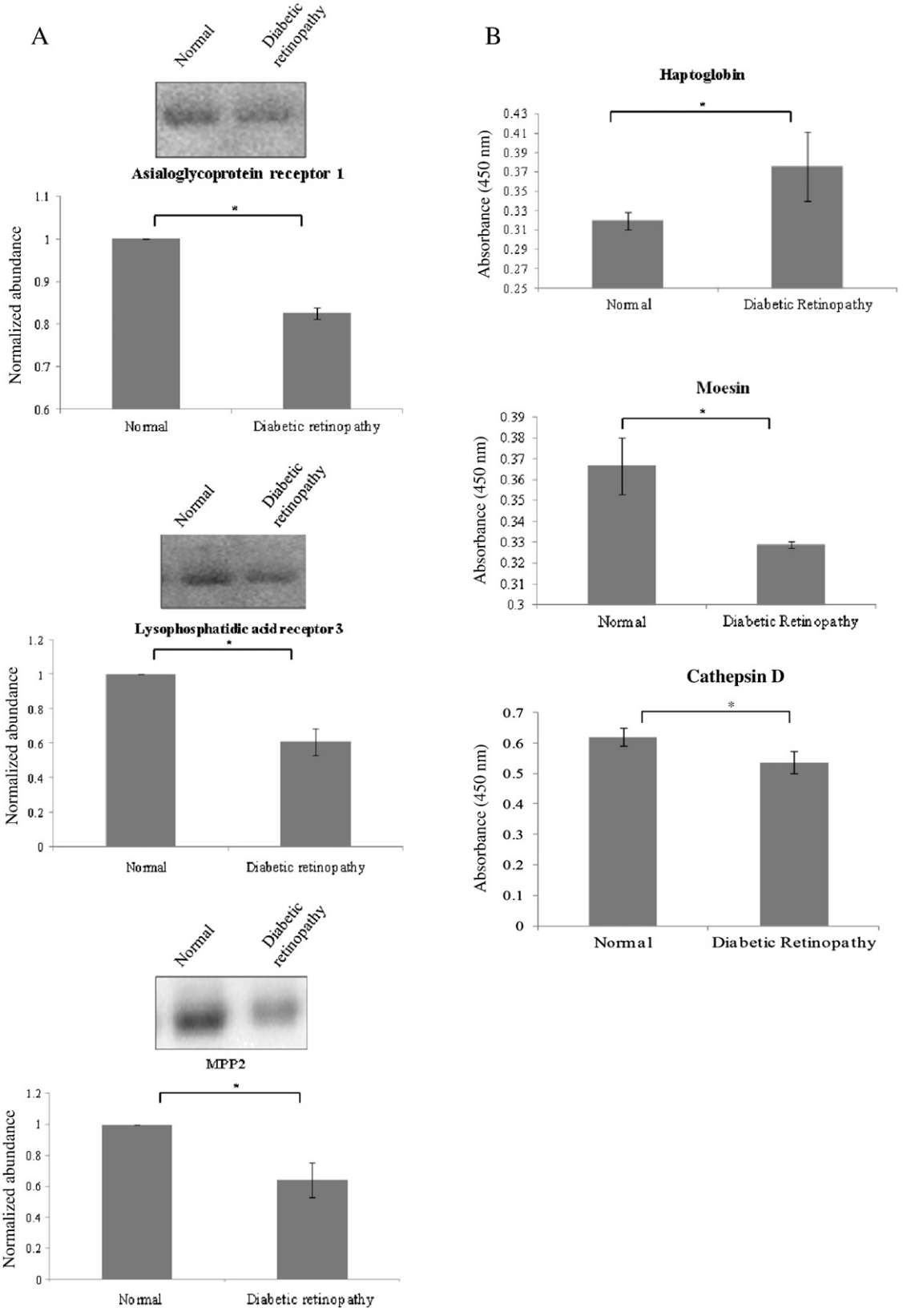

Fig. 9 – Representative immunoblotting and ELISA analysis of asialoglycoprotein receptor 1, lysophosphatidic acid receptor 3, MPP2, haptoglobin, moesin and cathepsin D in plasma from type 2 diabetic patients with retinopathy and healthy donors. Plasma samples from 15 type 2 diabetic retinopathy patients and 15 healthy donors were run in a pool. (A) 30 μg of plasma samples were loaded and resolved by SDS-PAGE followed by immunoblotted against asialoglycoprotein receptor 1, lysophosphatidic acid receptor 3 and MPP2. (B) 50 μg of plasma samples were coated onto each well of 96-well plate for ELISA analysis against haptoglobin, moesin and cathepsin D and the absorbance was measured at 450 nm using a Stat Fax 2100 microtiterplate reader. *Signifies a p-value of ≦ 0.05.

cells and that its deficiency induces apoptosis of the retinal cells [42]. In high glucose concentration, the accumulation of advanced glycation end products has also been reported to cause a significant reduction in cathepsin D expression in ARPE-19 [43]. These previous observation agreed with our results and supported the model that high glucose-induced high amount of advanced glycation end products which subsequently down-regulated cathepsin D and lead to retinal cell apoptosis. On the other hand, no report demonstrates the relationship between identified protease, cathepsin L1, and diabetic retinopathy. The roles of cathepsin L1 in high glucose culture and diabetic retinopathy are warrant further investigation.

In *in vitro* study, 5.5 mM D-glucose corresponds to fasting plasma glucose level of type 1 DM-free people and 25/100 mM correspond to 2 h after meal plasma glucose level of diabetic patients and glucose level in uncontrolled diabetic patients, respectively. In clinical specimen analysis, normal controls largely have serum glucose around 5.5 mM; while, diabetic retinopathy patients have serum glucose ranging from 25 to 100 mM. Thus, 5.5 mM glucose cultured ARPE-19 cells were used to mimic normal controls; on the other hand, 25 and 100 mM glucose cultured ARPE-19 cells were used to mimic diabetic retinopathy. To compare clinical sample and *in vitro* validation, haptoglobin is up-regulated in both high glucose cultured ARPE-19 and diabetic retinopathy plasma; in contrast, MPP2 and cathepsin D are both down-regulated in high glucose cultured ARPE-19 and diabetic retinopathy plasma. Notably, cathepsin D displays a dramatically down-regulation in between 25 mM and 100 mM glucose cultured ARPE-19 as well as down-regulation in between normal control plasma and diabetic retinopathy plasma implying the average serum glucose concentrations of diabetic retinopathy patients are ranging from 25 mM to 100 mM glucose regardless of the other physiological factors. In general, the trends of these 3 proteins seem consistent between *in vitro* study and clinical specimen analysis.

In the current study, 2D-DIGE experiment is based on fluorescence-based secreted protein quantification which can detect sub-nanogram level of dye-labeled proteins; on the other hand, our post-staining experiment is based on modified colloidal coomassie blue staining with sensitivity around 20–50 ng [44]. Hence, numerous differentially expressed dye-labeled low-abundant secreted proteins can be detected by fluorescent scanner but failed to be visualized with colloidal coomassie blue staining. This is the reason why only around 70% differentially expressed secreted features on 2-DE can be picked for MALDI-TOF identification.

In conclusion, the quantitative plasma proteomics analysis based on 2D-DIGE and MALDI-TOF MS provided a valuable impact for diabetic retinopathy research. Our quantitative proteomic approach has identified 20 proteins which have been reported as plasma biomarkers of diabetic retinopathy. Additionally, we have presented 35 putative diabetic retinopathy signatures, which may be associated with the progression and development of the disease and has a potential to serve as a useful tool for monitoring the course of the disease. Our study indicated an entire network of identified secreted proteins in high glucose-treated retinal cells, and deduced their roles in the formation of diabetic retinopathy. The potential of utilizing these markers for screening and treating diabetic retinopathy warrants further investigation.

Supplementary related to this article can be found online at http://dx.doi.org/10.1016/j.jprot.2012.07.014.

Declaration of competing interests

The authors confirm that there are no conflicts of interest.

Acknowledgments

This work was supported by the NSC grant (100-2311-B-007-005) from the National Science Council, Taiwan and Toward word-class university project from National Tsing Hua University, Taiwan. Nano- and Micro-ElectroMechanical Systems-based Frontier Research on Cancer Mechanism, Diagnosis, and Treatment grant from National Tsing Hua University.

REFERENCES

[1] Dorchy H, Toussaint D. Early rupture of the blood-retina barrier in young diabetics. Initial functional disorder of retinopathy in type 1 diabetes in children and adolescents. Rev Med Brux 1984;5:319-31.
[2] van Reyk DM, Gillies MC, Davies MJ. The retina: oxidative stress and diabetes. Redox Rep 2003;8:187-92.
[3] Stitt AW. AGEs and diabetic retinopathy. Invest Ophthalmol Vis Sci 2010;51:4867-74.
[4] Gelisken F, Ziemssen F. Diabetic maculopathy. Diagnosis and treatment. Ophthalmologe 2010;107:773-86.
[5] Ehrlich R, Harris A, Ciulla TA, Kheradiya N, Winston DM, Wirostko B. Diabetic macular oedema: physical, physiological and molecular factors contribute to this pathological process. Acta Ophthalmol 2010;88:279-91.
[6] Crawford TN, Alfaro III DV, Kerrison JB, Jablon EP. Diabetic retinopathy and angiogenesis. Curr Diabetes Rev 2009;5:8–13.
[7] Girach A, Lund-Andersen H. Diabetic macular oedema: a clinical overview. Int J Clin Pract 2007;61:88-97.
[8] Huang HL, Hsing HW, Lai TC, Chen YW, Lee TR, Chan HT, et al. Trypsin-induced proteome alteration during cell subculture in mammalian cells. J Biomed Sci 2010;17:36.
[9] Lai TC, Chou HC, Chen YW, Lee TR, Chan HT, Shen HH, et al. Secretomic and proteomic analysis of potential breast cancer markers by two-dimensional differential gel electrophoresis. J Proteome Res 2010;9:1302-22.
[10] Wu CL, Chou HC, Cheng CS, Li JM, Lin ST, Chen YW, et al. Proteomic analysis of UVB-induced protein expression- and redox-dependent changes in skin fibroblasts using lysine- and cysteine-labeling two-dimensional difference gel electrophoresis. J Proteomics 2012;75:1991-2014.
[11] Chen YW, Chou HC, Lyu PC, Yin HS, Huang FL, Chang WS, et al. Mitochondrial proteomics analysis of tumorigenic and metastatic breast cancer markers. Funct Integr Genomics 2011;11:225-39.
[12] Chou HC, Chen YW, Lee TR, Wu FS, Chan HT, Lyu PC, et al. Proteomics study of oxidative stress and Src kinase inhibition in H9C2 cardiomyocytes: a cell model of heart ischemia reperfusion injury and treatment. Free Radic Biol Med 2010;49:96–108.

[13] Mannermaa E, Reinisalo M, Ranta VP, Vellonen KS, Kokki H, Saarikko A, et al. Filter-cultured ARPE-19 cells as outer blood-retinal barrier model. Eur J Pharm Sci 2010;40:289-96.
[14] Glotin AL, Debacq-Chainiaux F, Brossas JY, Faussat AM, Treton J, Zubielewicz A, et al. Prematurely senescent ARPE-19 cells display features of age-related macular degeneration. Free Radic Biol Med 2008;44:1348-61.
[15] Garcia-Ramirez M, Villarroel M, Corraliza L, Hernandez C, Simo R. Measuring permeability in human retinal epithelial cells (ARPE-19): implications for the study of diabetic retinopathy. Methods Mol Biol 2011;763:179-94.
[16] Candiloros H, Muller S, Zeghari N, Donner M, Drouin P, Ziegler O. Decreased erythrocyte membrane fluidity in poorly controlled IDDM. Influence of ketone bodies. Diabetes Care 1995;18:549-51.
[17] Saydah SH, Miret M, Sung J, Varas C, Gause D, Brancati FL. Postchallenge hyperglycemia and mortality in a national sample of U.S. adults. Diabetes Care 2001;24:1397-402.
[18] Jouven X, Lemaitre RN, Rea TD, Sotoodehnia N, Empana JP, Siscovick DS. Diabetes, glucose level, and risk of sudden cardiac death. Eur Heart J 2005;26:2142-7.
[19] Cai L, Li W, Wang G, Guo L, Jiang Y, Kang YJ. Hyperglycemia-induced apoptosis in mouse myocardium: mitochondrial cytochrome C-mediated caspase-3 activation pathway. Diabetes 2002;51:1938-48.
[20] Chan HL, Gharbi S, Gaffney PR, Cramer R, Waterfield MD, Timms JF. Proteomic analysis of redox- and ErbB2-dependent changes in mammary luminal epithelial cells using cysteine- and lysine-labelling two-dimensional difference gel electrophoresis. Proteomics 2005;5:2908-26.
[21] Chou HC, Lu YC, Cheng CS, Chen YW, Lyu PC, Lin CW, et al. Proteomic and redox-proteomic analysis of berberine-induced cytotoxicity in breast cancer cells. J Proteomics 2012;75:3158-76.
[22] Izuta H, Matsunaga N, Shimazawa M, Sugiyama T, Ikeda T, Hara H. Proliferative diabetic retinopathy and relations among antioxidant activity, oxidative stress, and VEGF in the vitreous body. Mol Vis 2010;16:130-6.
[23] Xue H, Lu B, Lai M. The cancer secretome: a reservoir of biomarkers. J Transl Med 2008;6:52.
[24] Yamaguchi N, Yamamura Y, Koyama K, Ohtsuji E, Imanishi J, Ashihara T. Characterization of new human pancreatic cancer cell lines which propagate in a protein-free chemically defined medium. Cancer Res 1990;50:7008-14.
[25] Inoue Y, Kawamoto S, Shoji M, Hashizume S, Teruya K, Katakura Y, et al. Properties of ras-amplified recombinant BHK-21 cells in protein-free culture. Cytotechnology 2000;33: 21-6.
[26] Jacobs JM, Mottaz HM, Yu LR, Anderson DJ, Moore RJ, Chen WN, et al. Multidimensional proteome analysis of human mammary epithelial cells. J Proteome Res 2004;3:68-75.
[27] Koike M, Shibata M, Ohsawa Y, Nakanishi H, Koga T, Kametaka S, et al. Involvement of two different cell death pathways in retinal atrophy of cathepsin D-deficient mice. Mol Cell Neurosci 2003;22:146-61.
[28] Bollineni JS, Alluru I, Reddi AS. Heparan sulfate proteoglycan synthesis and its expression are decreased in the retina of diabetic rats. Curr Eye Res 1997;16:127-30.
[29] Ringvall M, Kjellen L. Mice deficient in heparan sulfate N-deacetylase/N-sulfotransferase 1. Prog Mol Biol Transl Sci 2010;93:35-58.
[30] Grobe K, Ledin J, Ringvall M, Holmborn K, Forsberg E, Esko JD, et al. Heparan sulfate and development: differential roles of the N-acetylglucosamine N-deacetylase/N-sulfotransferase isozymes. Biochim Biophys Acta 2002;1573:209-15.
[31] Ringvall M, Ledin J, Holmborn K, van Kuppevelt T, Ellin F, Eriksson I, et al. Defective heparan sulfate biosynthesis and neonatal lethality in mice lacking N-deacetylase/N-sulfotransferase-1. J Biol Chem 2000;275: 25926-30.
[32] Khalfaoui T, Lizard G, Beltaief O, Colin D, Ben Hamida J, Errais K, et al. Immunohistochemical analysis of cellular adhesion molecules (ICAM-1, VCAM-1) and VEGF in fibrovascular membranes of patients with proliferative diabetic retinopathy: preliminary study. Pathol Biol (Paris) 2009;57: 513-7.
[33] Khalfaoui T, Lizard G, Ouertani-Meddeb A. Adhesion molecules (ICAM-1 and VCAM-1) and diabetic retinopathy in type 2 diabetes. J Mol Histol 2008;39:243-9.
[34] Kamiuchi K, Hasegawa G, Obayashi H, Kitamura A, Ishii M, Yano M, et al. Intercellular adhesion molecule-1 (ICAM-1) polymorphism is associated with diabetic retinopathy in Type 2 diabetes mellitus. Diabet Med 2002;19:371-6.
[35] Lumeng C, Phelps S, Crawford GE, Walden PD, Barald K, Chamberlain JS. Interactions between beta 2-syntrophin and a family of microtubule-associated serine/threonine kinases. Nat Neurosci 1999;2:611-7.
[36] Meng W, Mushika Y, Ichii T, Takeichi M. Anchorage of microtubule minus ends to adherens junctions regulates epithelial cell-cell contacts. Cell 2008;135:948-59.
[37] Shelton L, Rada JA. Inhibition of human scleral fibroblast cell attachment to collagen type I by TGFBIp. Invest Ophthalmol Vis Sci 2009;50:3542-52.
[38] Ziyadeh FN, Fumo P, Rodenberger CH, Kuncio GS, Neilson EG. Role of protein kinase C and cyclic AMP/protein kinase A in high glucose-stimulated transcriptional activation of collagen alpha 1 (IV) in glomerular mesangial cells. J Diabetes Complications 1995;9:255-61.
[39] Miles AJ, Skubitz AP, Furcht LT, Fields GB. Promotion of cell adhesion by single-stranded and triple-helical peptide models of basement membrane collagen alpha 1(IV)531-543. Evidence for conformationally dependent and conformationally independent type IV collagen cell adhesion sites. J Biol Chem 1994;269:30939-45.
[40] Tsukita S. ERM (ezrin/radixin/moesin) as crosslinkers between actin filaments and plasma membranes. Tanpakushitsu Kakusan Koso 1996;41:1899-905.
[41] Ivanova S, Gregorc U, Vidergar N, Javier R, Bredt DS, Vandenabeele P, et al. MAGUKs, scaffolding proteins at cell junctions, are substrates of different proteases during apoptosis. Cell Death Dis 2011;2:e116.
[42] Strauss O. The retinal pigment epithelium in visual function. Physiol Rev 2005;85:845-81.
[43] Glenn JV, Mahaffy H, Wu K, Smith G, Nagai R, Simpson DA, et al. Advanced glycation end product (AGE) accumulation on Bruch's membrane: links to age-related RPE dysfunction. Invest Ophthalmol Vis Sci 2009;50:441-51.
[44] Chan HL, Gharbi S, Gaffney PR, Cramer R, Waterfield MD, Timms JF. Proteomic analysis of redox- and ErbB2-dependent changes in mammary luminal epithelial cells using cysteine- and lysine-labelling two-dimensional difference gel electrophoresis. Proteomics 2005;5:2908-26.